Supporting information

Hierarchical Mesoporous Selenium@Bimetallic Selenides Quadrilateral Nanosheets Array for Advanced Flexible Asymmetric Supercapacitor

*Yan Zhao [a, c], Sichao Wang [c], Fei Ye [b], Wenjie Liu [c], Jiabiao Lian [c], Guochun Li [c], Huanting Wang [d], Linfeng Hu *[b], Limin Wu *[a, e]*

[a] College of Chemistry and Chemical Engineering, Inner Mongolia University, Hohhot, 010021 China

[b] School of Materials Science and Engineering, Southeast University Nanjing, 211189 China

[c] Institute for Energy Research, Jiangsu University, Zhenjiang, 212013 China

[d] Department of Chemical Engineering, Monash University, Victoria, 3800, Australia

[e] Department of Materials Science, Fudan University, Shanghai, 200433, China

* Corresponding authors: lmw@fudan.edu.cn; linfenghu@seu.edu.cn

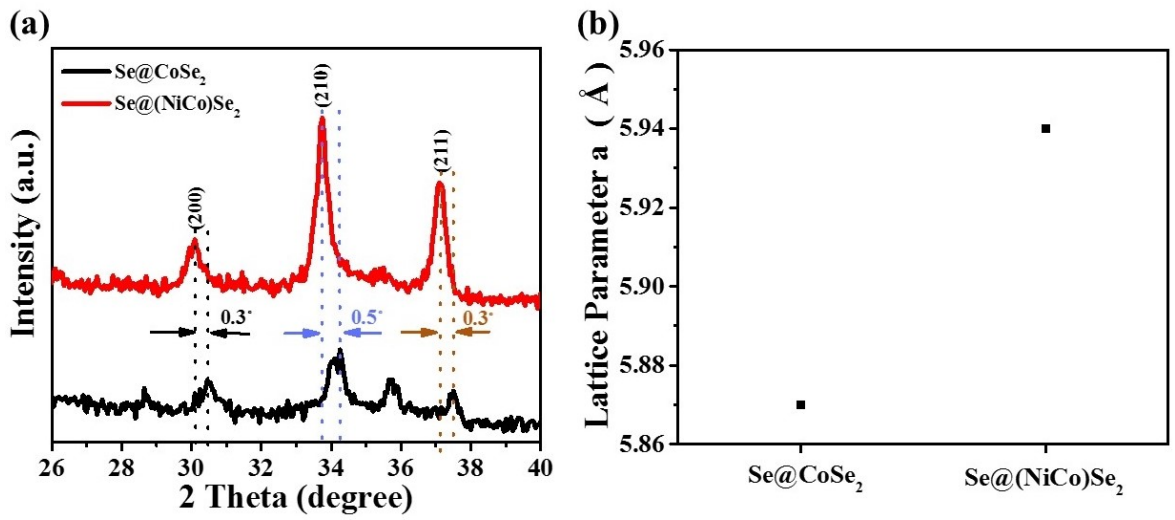

Figure S1. (a) The XRD patterns of $Se@CoSe_2$ and $Se@(NiCo)Se_2$ range from 26° to 40°. (b) The lattice parameter of $Se@CoSe_2@Se$ and $Se@(NiCo)Se_2$.

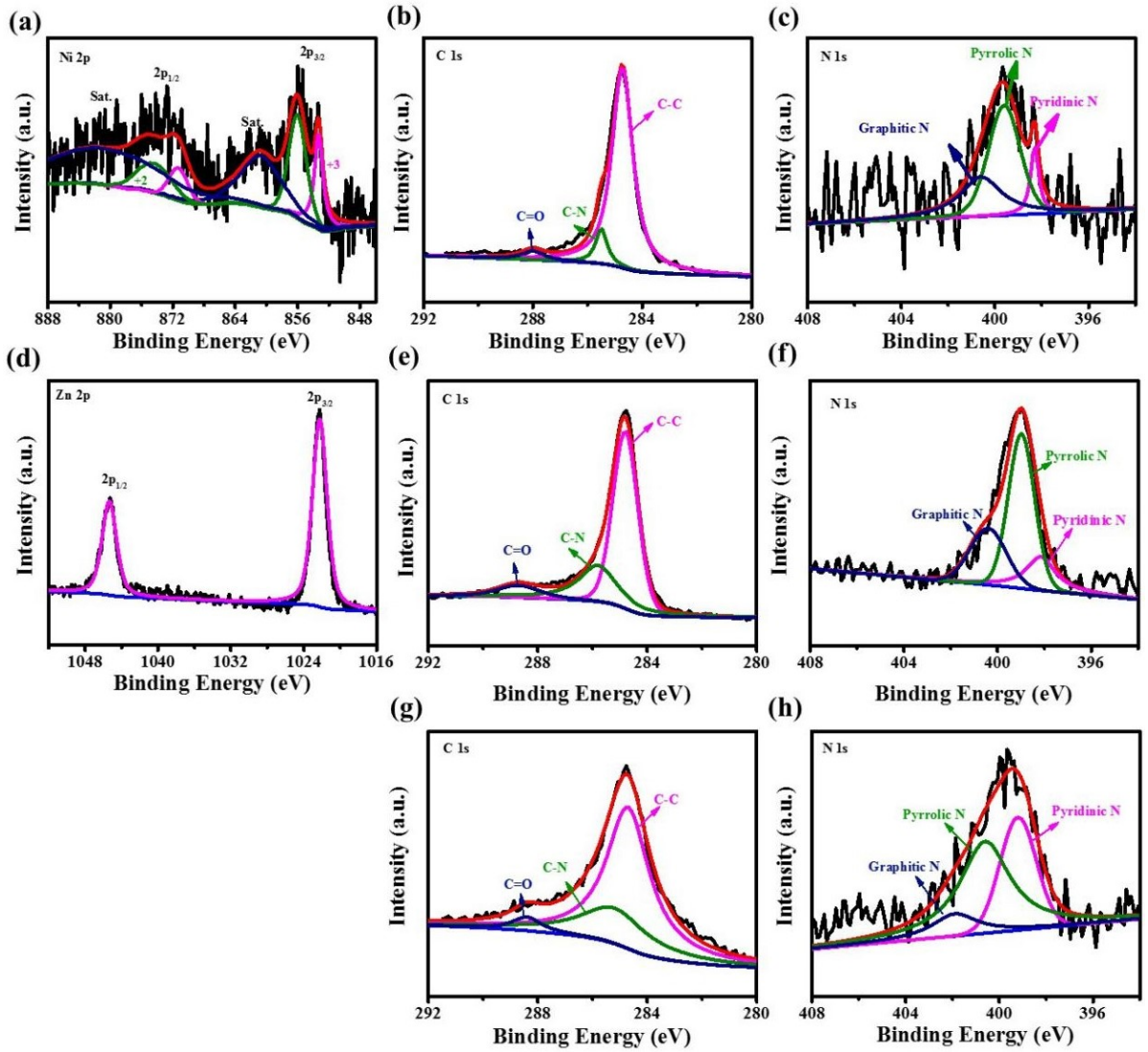

Figure S2. (a) Ni 2p, (b) C 1s, and (c) N 1s XPS spectra of Se@(NiCo)Se_2. (d) Zn 2p, (e) C 1s, and (f) N 1s XPS spectra of Se@(ZnCo)Se_2. (g) C 1s, and (h) N 1s XPS spectra of Se@$CoSe_2$.

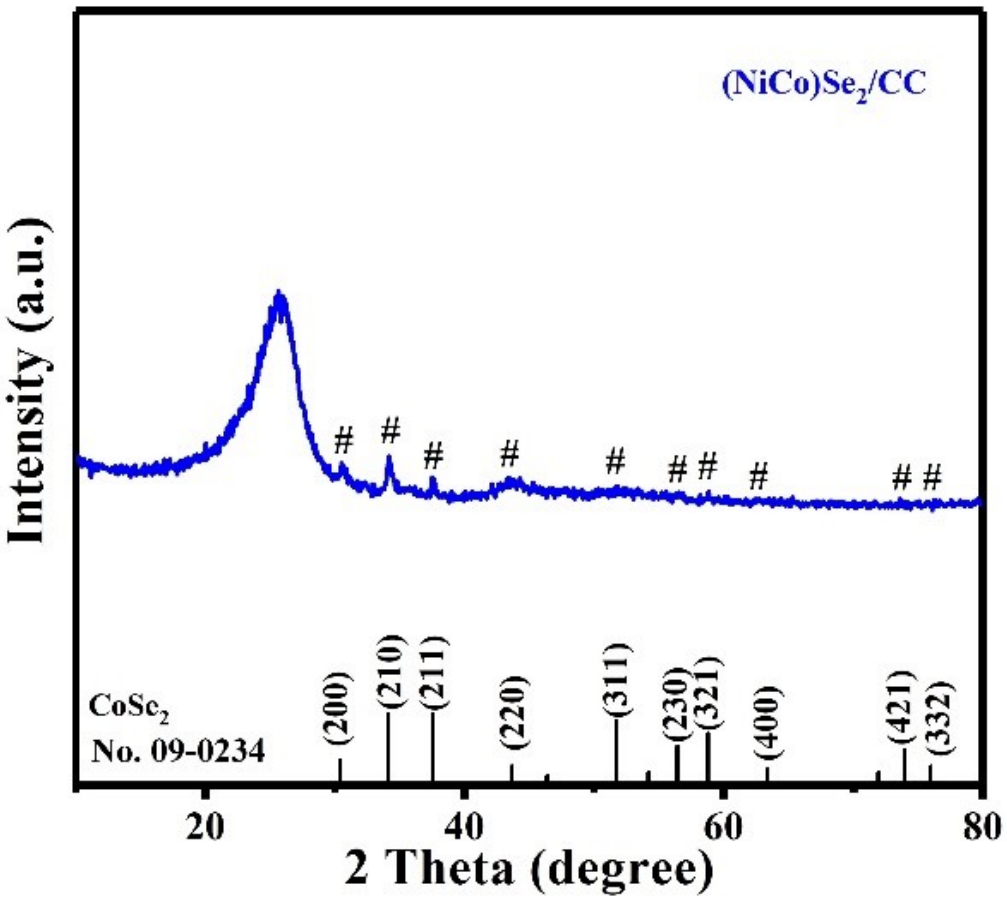

Figure S3. XRD pattern of the post-processed (NiCo)Se_2/CC sample.

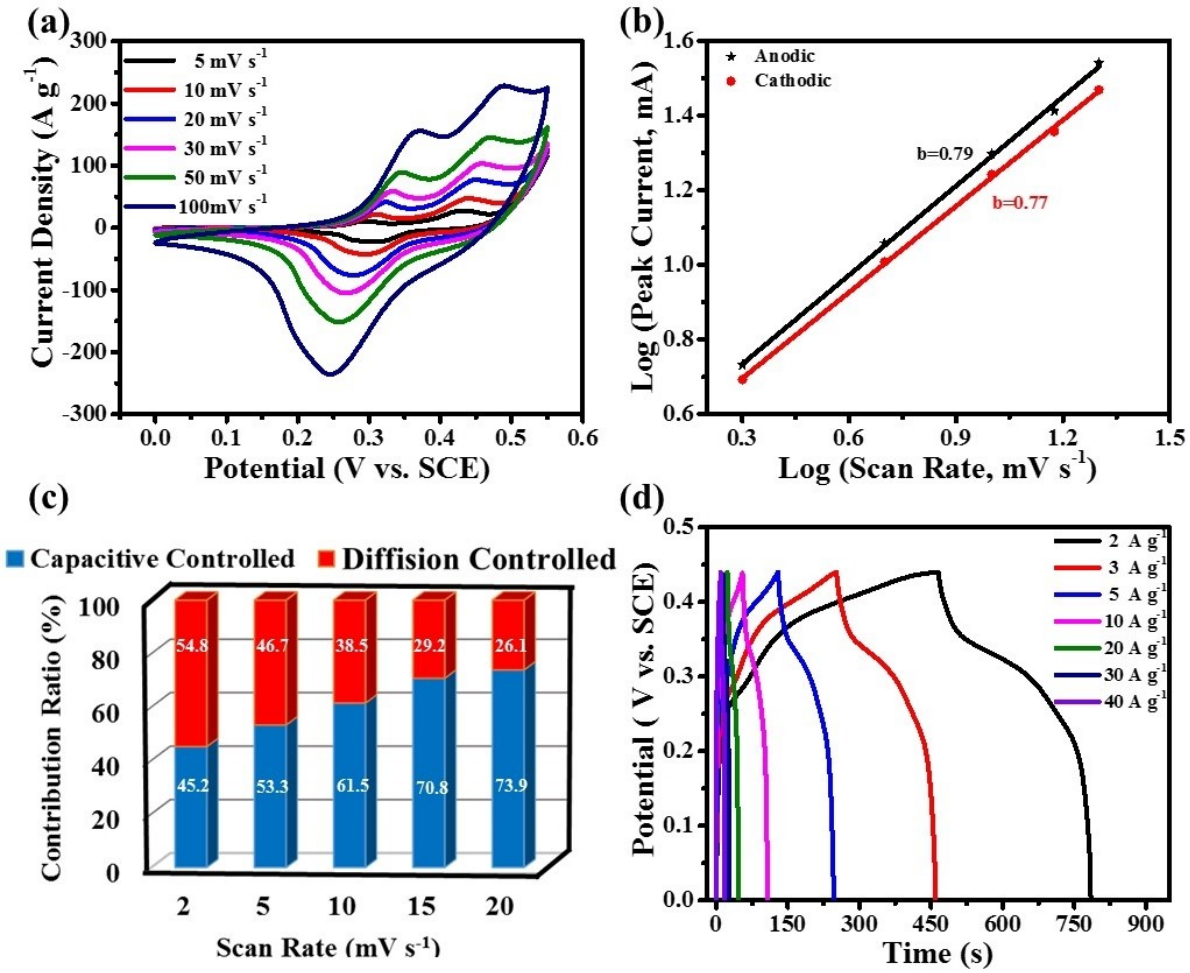

Figure S4. (a) CV curves, (b) Log (Peak Current) *vs*. log (Scan Rate) plots of Se@(NiCo)Se_2/CC, (c) Illustration of the possible capacity contribution ratios at different scan rates, and (d) GCD curves of the Se@(NiCo)Se_2/CC electrode.

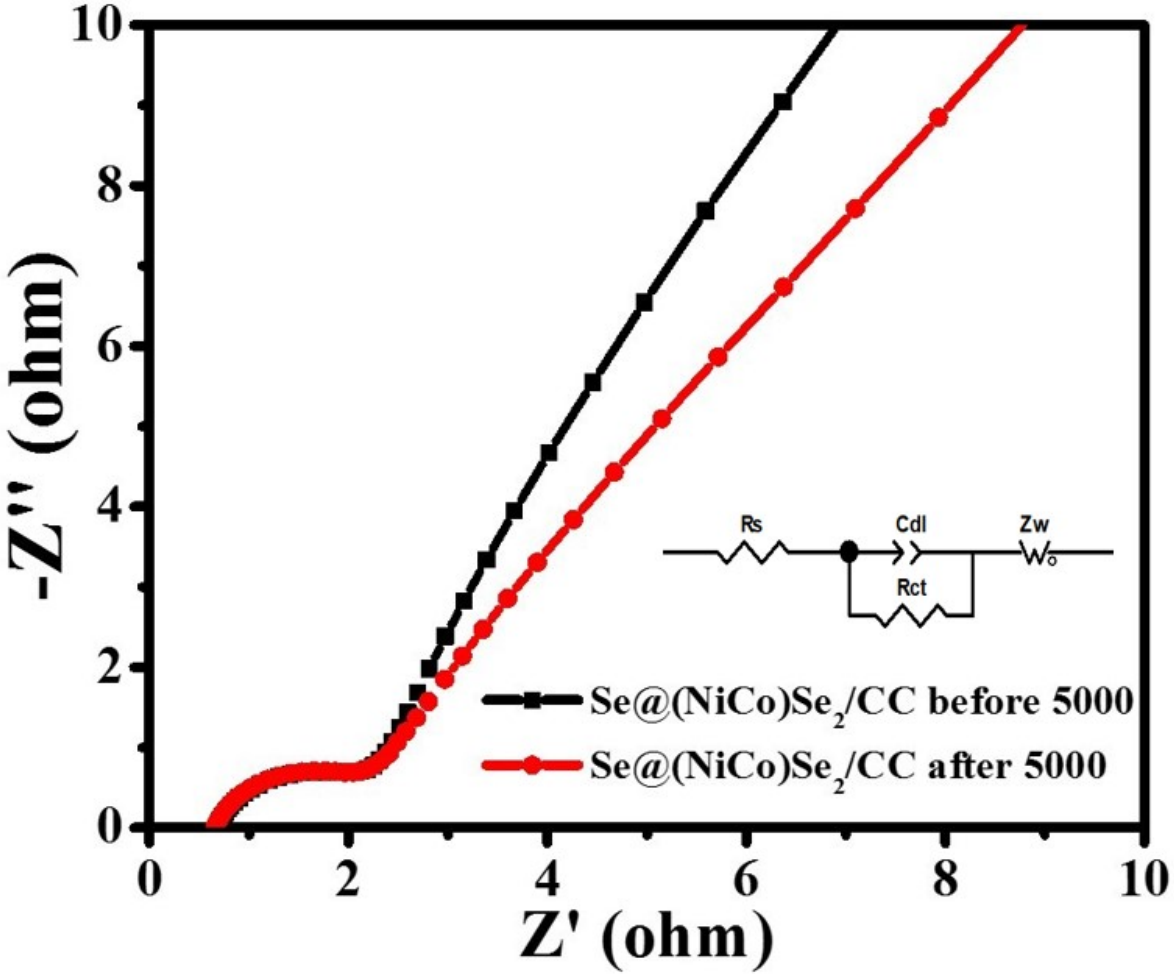

Figure S5. EIS curves of the Se@(NiCo)Se_2/CC electrode before and after cycling at a current density of 20 A g^{-1} recorded at open-circuit potentials.

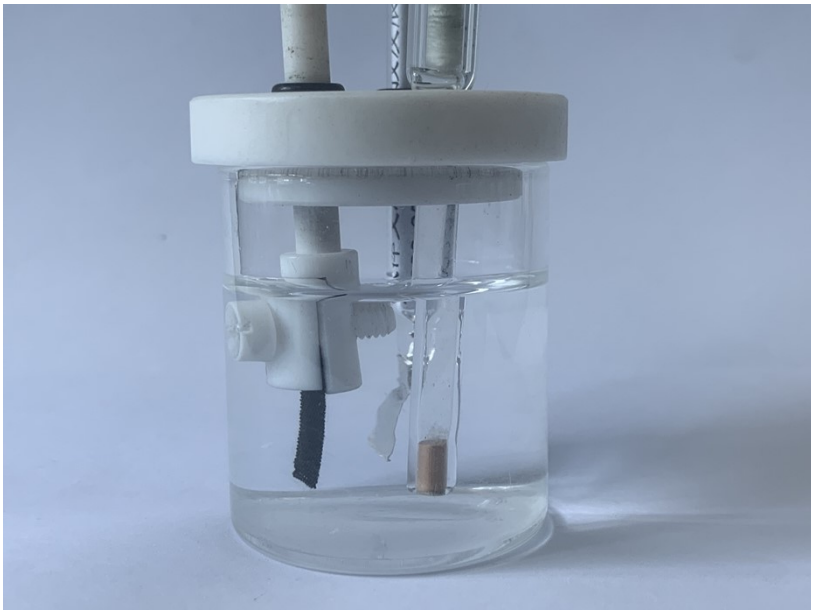

Figure S6. Photograph of the closed reaction equipment in a three-electrode system.

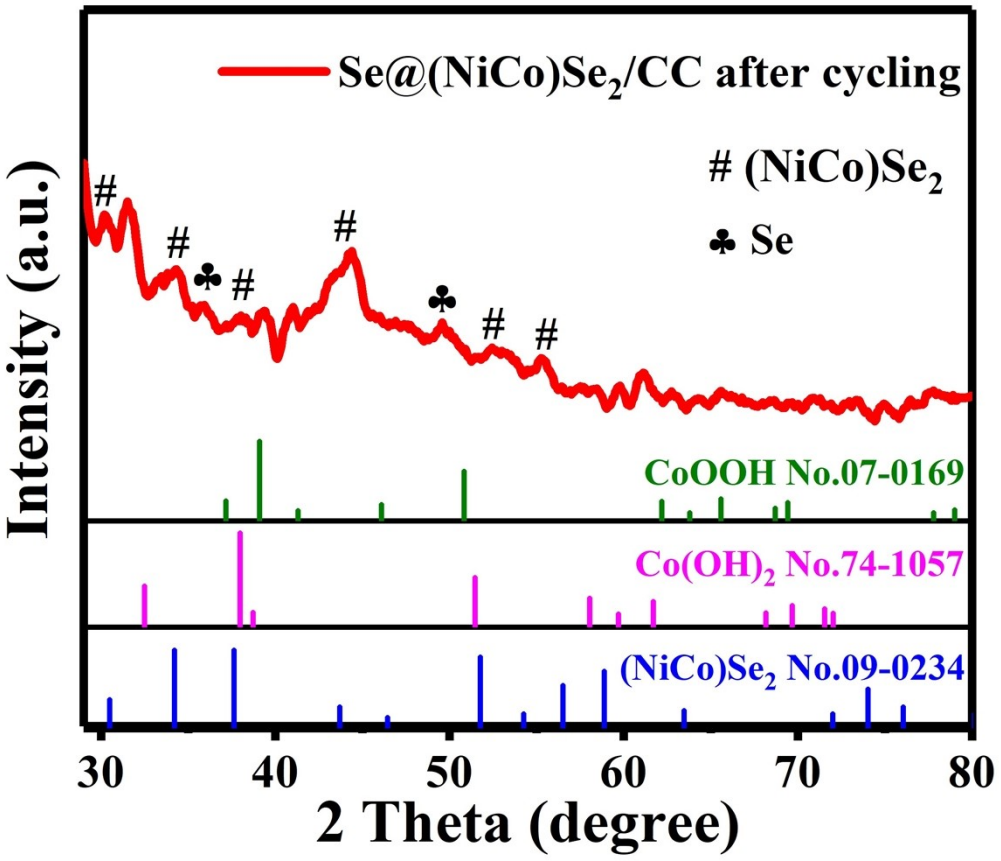

Figure S7. XRD pattern of the Se@(NiCo)Se_2 electrode after cycling test.

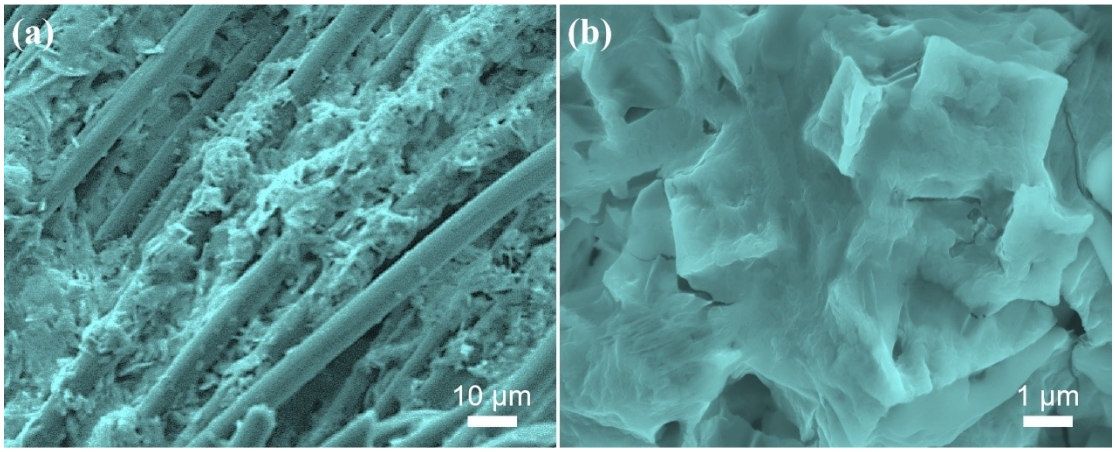

Figure S8. SEM images of the Se@(NiCo)Se_2/CC electrode after cycling test.

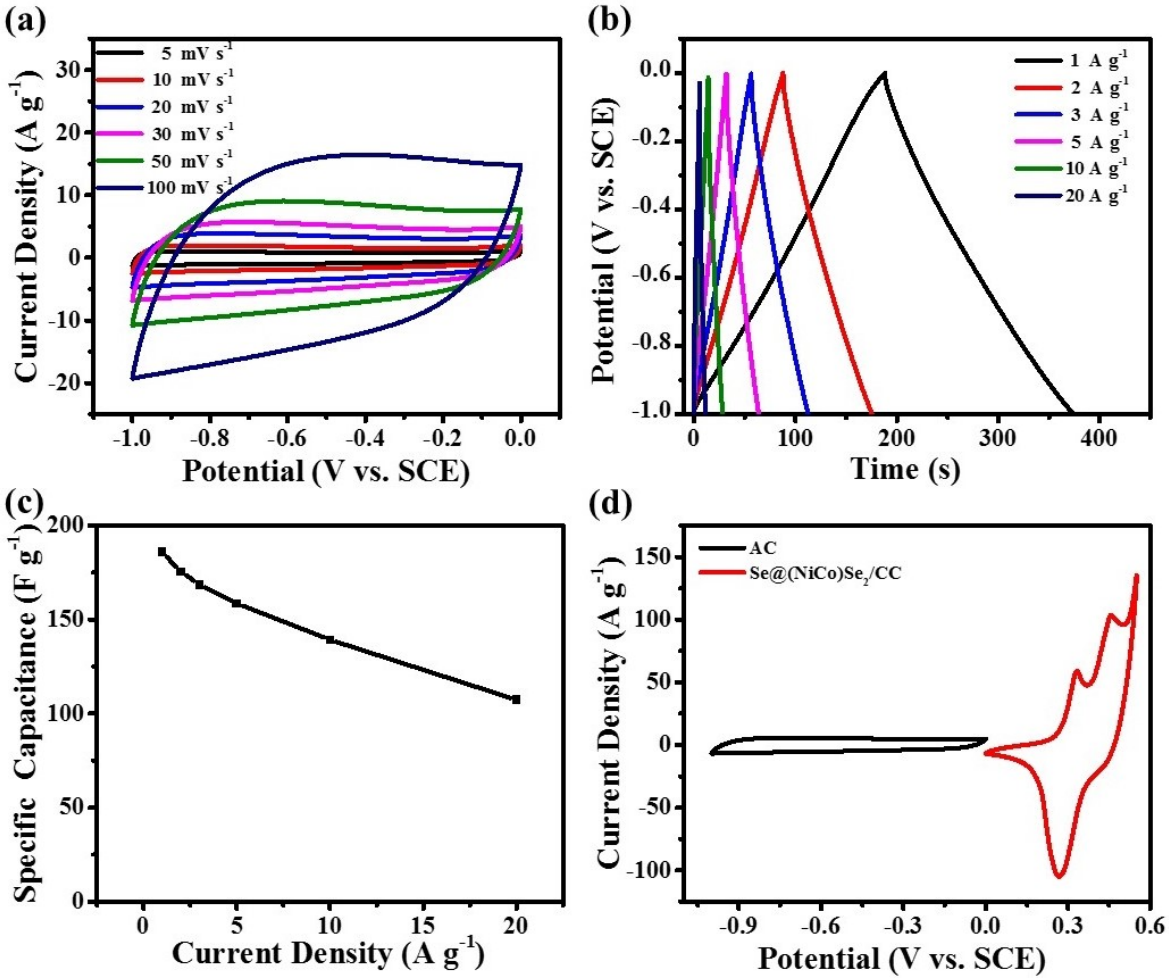

Figure S9. (a) CV, (b)GCD, and (c) Specific capacitance of AC electrode. (d) CV curves (scan rate of 30 mV s^{-1}) of AC and Se@(NiCo)Se_2/CC electrodes.

Table S1. The comparison of the specific capacitance, potential windows, electrolyte, and rate capability of the Se@(NiCo)Se_2 electrode and the related work in literature.

Electrode materials	***C_s* (F g^{-1})**	**Potential windows (V)**	**Electrolyte**	**Rate capability**	**Ref.**
$CoSe_2$/rGO	219 (0.5 A g^{-1})	-0.2-0.45	3M KOH	0.5-10 A g^{-1} 73 %	42
$CoSe_2$/NC	1236.34 (1 A g^{-1})	0-0.35	6 M KOH	1-20 A g^{-1} 61.2 %	43
Porous $CoSe_2$/NF	713.2 (1 mA cm^{-2})	-0.1-0.4	3 M KOH	1-20 mA cm^{-2} 75.1 %	44
2D CoSNC	360.1 (1.5 A g^{-1})	0-0.6	2 M KOH	1-30 A g^{-1} 56.8 %	17
Cu-TCPP@PPy	500 (1 A g^{-1})	-0.2-0.7	2 M KOH	1-10 A g^{-1} 57 %	45
Co-TCPP Nanosheet/GO	510 (5 A g^{-1})	-0.1-0.4	6 M KOH	5-20 A g^{-1} 74.5 %	16
H-$NiCoSe_2$ sub-microspheres	750 (3 A g^{-1})	-0.2-0.4	6 M KOH	44.0 % 3-30 A g^{-1}	46
$Ni_{0.6}Co_{0.4}Se_2$	1339.1 (1 A g^{-1})	0-0.45	6 M KOH	1-20 A g^{-1} 77.7 %	9
Se@(NiCo)Se_2/CC	**1920 (2 A g^{-1})**	**0-0.45**	**3M KOH**	**2-40 A g^{-1} 55.5 %**	**This work**

rGO: reduced graphene oxide, NC: N-doped carbon, NF: nickel foam, CoSNC: $CoS_{1.097}$ nanoparticles and nitrogen-doped carbon, PPy: polypyrrole, GO: graphene oxide, H: Hollow, CC: carbon cloth

Table S2. Comparison of energy and power densities of our Se@(NiCo)Se_2//AC asymmetric supercapacitor with the related work in literature.

Hybrid supercapacitors	Energy density Wh kg^{-1}	Power density W kg^{-1}	Reference
$Ni_{0.6}Co_{0.4}Se_2$//BNPC	14.5	16300	9
$CoSe_2$/NC-NF//AC	40.9	980	43
H-$NiCoSe_2$//AC	25.5	3750	46
NiCo-MOF//AC	20.9	800	60
Ni-MOF//AC	31.5	800	61
$CoSe_2$ nanoarrays//carboon nanowall	32.2	1914.7	62
Se@(NiCo)Se_2//AC	**49.4**	**787.3**	**This work**

AC: activated carbon, BNPC: boron and nitrogen co-doped porous carbon foam, NC: N-doped carbon, NF: nickel foam.